Catalysis Today 124 (2007) 71-79

Oxidation of methanol on Ru catalyst: Effect of the reagents partial pressures on the catalyst oxidation state and selectivity

R. Blume [a], M. Hävecker [a], S. Zafeiratos [a], D. Teschner [a], A. Knop-Gericke [a], R. Schlögl [a], P. Dudin [b], A. Barinov [b], M. Kiskinova [b]*

[a] Fritz-Haber-Institut der Max-Planck-Gesellschaft, Faradayweg 4-6, 14195 Berlin, Germany
[b] Sincrotrone Trieste, AREA Science Park, Basovizza, Trieste 34012, Italy

* Corresponding author: e-mail Maya.Kiskinova@elettra.trieste.it,

Available online 2. April 2007.

Abstract

In situ core level photoelectron spectroscopy and mass spectrometry have been utilized to study the methanol oxidation on a model RuO2 catalyst at pressures ranging from 10^{-6} to 10^{-1} mbar. The experiments were carried out varying the O_2/CH_3OH molecular mixing ratio from 0.25 to 3.3 and the reaction temperature from 350 to 720 K. The Ru $3d_{5/2}$ and O 1s core level spectra were used to characterise the dynamic changes in the Ru oxidation state by exposing the oxide pre-catalyst to different reagents partial pressures and temperatures. Full oxidation to $CO_2 + H_2O$ or partial oxidation to $CO + H_2O + H_2$ have been observed in the whole pressure range for specific reaction conditions, which preserve the oxide catalyst state or reduce the oxide to metallic Ru. The selective oxidation to formaldehyde is observed only at pressures in the 10^{-1} mbar range, catalyzed by a RuOx surface oxide formed by partial reduction of the oxide pre-catalyst.

Keywords: Ruthenium; Methanol; Oxidation; Formaldehyde; High-pressure XPS; Mass-spectrometry

1. Introduction

The catalytically active state under reaction conditions is still a very disputable issue. In the particular cases of oxidation reactions the classical oxygen source considered in modelling the reactions mechanism is the lattice oxygen on nearly stoichiometric surfaces of metal oxides (Mars–van Krevelen mechanism) [1], or adsorbed oxygen on metal surfaces. In both cases, the consumed surface oxygen is restored by the O_2 reactant in the gas phase.

In reality, the catalytically active state is not necessarily the well-defined oxide phase, and possible differences in the socalled 'oxidation state' of the surface and the bulk have already been considered [2]. Studies of selective oxidation of CH_3OH on Cu have provided clear evidence for catalytically active state with incorporated subsurface oxygen, which can be described as a disordered surface oxide film [3,4]. Such surface oxide states are in fact the transient precursors towards formation of metal bulk oxides, which nucleate and grow when a critical amount of oxygen is incorporated subsurface [5]. The calculated temperature–pressure (T, P_{O2}) phase diagrams attempting to predict the thermodynamically stable phases under realistic oxidation conditions confirm that the oxidation of transition metals is a rather complex process with phase coexistence regions [6–8]. In realistic oxidation reactions the second reactant usually acts as a reducer (e.g. CO, H_2, CH_3OH or other organic molecules) and affects the (T, P_{O2}) space of oxidation phases driving the oxidation state away from the equilibrium achieved in a pure O_2 ambient. Consequently, when the reactions have several possible pathways the selectivity and the corresponding catalytically active state can be controlled by varying the reaction temperature and chemical potentials (partial pressures) of the reactants.

In the last decade a main challenge of the surface science UHVexperiments is that often enough the extensive knowledge about important elementary processes at the model catalyst's surface cannot be directly extrapolated to the catalytic processes occurring at ambient pressures, when the chemical potentials of reagents in the gas phase become important. In this respect Ru, a catalyst used in exhaust gas converters and fuel cells is a textbook example of the so-called 'pressure gap' in oxidation and catalyst activity. Under UHV conditions the Ru catalyst turned out

to be completely inactive for CO oxidation due to the kinetic limitation for accumulation of oxygen to form the catalytically active surface at the low oxygen potentials in the traditional surface science experiments [9–11]. The crucial role of the PO2 became apparent in a number of recent investigations showing that it is a prerequisite for formation of the catalytically active phases, namely a thin surface oxide film (RuOx) at T < 550 K and a stoichiometric well-ordered RuO2(1 1 0) phase at T > 550 K [10,12–14]. Extensive structural, photoemission and TPD studies characterized the lower temperature Ru oxidation state as a disordered RuOx with 1–4 ML oxygen incorporated within the top few Ru layers, which also precedes the nucleation and growth of the stoichiometric RuO2 phase at higher temperatures [14]. They have also provided evidence for the coexistence of RuOx with the RuO2 phase in a wide (T, PO2) range.

One of the approaches to narrowing the pressure gap, used in our previous study of CO oxidation on a Ru(0001) catalyst, is monitoring the catalytically active state and products in the gas phase by in situ mbar–bar pressure X-ray photoemission spectroscopy (XPS) and mass-spectrometry [3]. We found that below 500 K, when the formation of RuO_2 is kinetically hindered, the surface is already activated for CO oxidation by formation of the precursor surface oxide, RuOx [15]. The actual surface state of the catalyst dynamically changed with temperature and CO/O_2 partial pressures. Both the RuOx 'surface oxide' and RuO_2 states can easily be reduced into an inactive Ru metal with adsorbed oxygen in excess of CO and Ru can be re-oxidised in an excess of oxygen regaining the catalytic activity. The active role of subsurface oxygen and formation of surface oxide RuOx have also been considered in catalytic behaviour of Ru electrodes in fuel cells [16,17].

The CO oxidation is a simple single-channel reaction system, which cannot tackle the 'pressure gap' in catalyst selectivity, another very important issue addressed by the present study of CH_3OH oxidation on a model Ru(0001) catalyst. CH_3OH catalytic oxidation is a complex process with long list of possible reactions involving different intermediates and final products, which also depend on the catalyst chemical state [18,19]. The first common step on both metal and oxide surfaces is H abstraction, yielding H_s or OH_s and methoxy, CH_3Os, where the subscript 's' indicates that the species is bonded at the surface. In the presence of oxygen further activation of the C–H bonds in CH_3O_s through red-ox cycles leading to H_2, CH_2O, CO, CO_2 and H_2O (products of partial or complete oxidation), passes through the following principle intermediates: OH_s, H_s, CH_xO_s, CO_s and $HCOO_s$. The CO_2 can result of decomposition of the $HCOO_s$ or secondary oxidation reaction of CO_s. Starting with an oxidised Ru(0001) catalyst, considered to be the catalytic active state for CH_3OH oxidative-dehydrogenation to $CH_2O + H_2O$ [20], we followed in real time the products yield and the evolution of Ru oxidation state and adlayer in the 10^{-6} to 10^{-1} mbar range varying the (T, PO_2 , PCH_3OH) space.

2 Experimental

The experiments were performed at the synchrotron radiation facility BESSY in Berlin in the high pressure XPS station designed and constructed in the FHI-MPG [21]. The sample, mounted inside a reaction cell, 2 mm away from the entrance aperture to the differentially pumped hemispherical analyser Phoibos 150 (SPECS GmbH), was heated from the backside using an infrared laser system. The CH_3OH and O_2 gas flows and the products released in the gas phase were monitored by a Hiden mass spectrometer. The fragmentation patterns of the reactants and products and the sensitivity factors were considered in the determination the molecular mixing ratio of the reagents and the relative yield of the products. In particular, this concerns the CH_2O and CO yields, which should be corrected for the attenuation of the CH_3OH-related mass signals 30 and 28 due to CH_3OH consumption. The relative decrease of the mass 31 was used as a measure of the methanol conversion. The Ru(0001) sample was cleaned before each reaction cycle using the well established procedures [12,22] and then oxidised to form a RuO_2 phase with thickness of 5–10 nm. All photoelectron spectra were normalized to the photon flux, monitored by a photodiode. The Ru 3d and O 1s spectra were measured in normal emission with photon energies of 450 and 650 eV, respectively and overall spectral resolution of 0.3 eV. According to the universal curve for the electron mean free path [23] the effective escape depths for the O 1s and Ru 3d photoelectrons is ~ 5 Å , which limits the probing depth to the top few layers (~ 10 Å).

The dynamic response of the O 1s and Ru $3d_{5/2}$ core level spectra was used for precise assignment of the catalyst oxidation state, which was correlated to the corresponding yields of the products of methanol oxidation. CO, CO_2, H_2, H_2O and CH_2O, detected with the mass spectrometer in our experiments. The already available Ru $3d_{5/2}$ and O 1s core level spectroscopy data provided the necessary basis for identification of the Ru oxidation states (metallic Ru with adsorbed oxygen, RuOx 'surface oxide', and RuO_2) and the ad-species (see Table 1). For the Ru(0001) surface the intensity ratio between the overlapping O-related Ru $3d_{5/2}$ component at 280.5–280.6 eV, accounting for both adsorbed oxygen and RuOx and the bulk component, Ru_{bulk}, turned out to be the best fingerprint for differentiation between adsorption oxygen state with coverage 0.33–0.67 ML on Ru(0001) and RuOx. For the RuOx state, detected under our experimental conditions this ratio was significantly higher for than the characteristic ratio of 0.3 for 0.67 ML of adsorbed oxygen and reaches ~ 0.6 for ~ 4 ML incorporated oxygen. The Ru $3d_{5/2}$ and O 1s spectra of the initial oxide pre-catalyst, prepared by in situ oxidation of Ru(0001) at 720 K and $10^{-1} < P_{O2} < 1$ mbar contained only the characteristic features of the RuO2 at 280.75 and 529.5 eV, respectively.

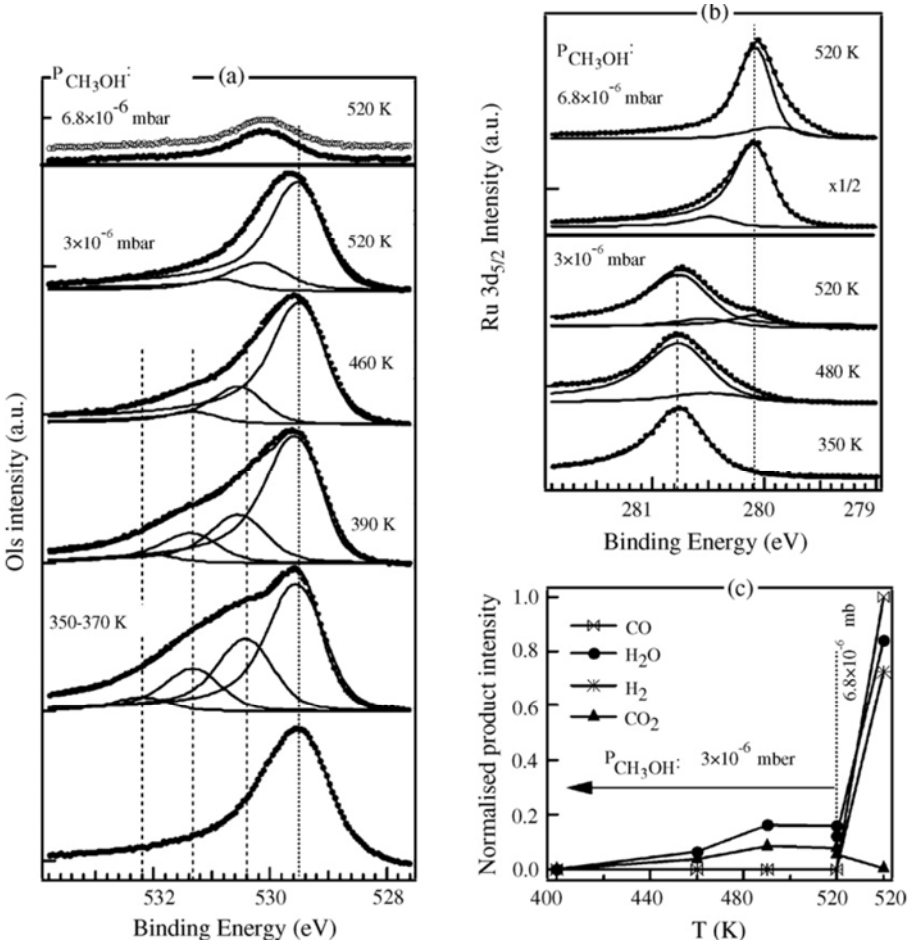

Fig. 1: O 1s (a) and Ru $3d_{5/2}$ (b) spectra taken at different temperatures for two different MR: 0.6 (bottom panel) and 0.25 (top panel). The bottom spectra in (a) and (b) represent the oxide pre-catalyst before introducing CH3OH in the gas phase. In (a) the dashed lines from left to right indicate the O 1s components assigned to CH2Os (_532.2), CH3Os (_531.5) and OHs (_530.5) and the dotted line indicates the oxide component. In (b) the dashed and dotted lines denote RuO2 and the Rubulk components. (c) Mass spectra normalized intensity of reaction products as a function of temperature and the changes occurring in products yield at 520 K after decreasing the MMR from 0.6 to 0.25. The dashed line divides the parts of different PCH3OH. PO2 was kept constant, 1.7 _ 10_6 mbar.

Table 1: Reported $Ru_{5/2}$ and O 1s binding energies of different chemical state of Ru and of some adsorbed species relevant to the present study

Core level	Binding energy (±0.05 eV)	Component identity	References
Ru $3d_{5/2}$	280.1	Ru(0 0 0 1)-bulk	[22,24]
Ru $3d_{5/2}$-	279.75	Ru(0 0 0 1)-surface	
Ru $3d_{5/2}$	280.75	RuO_2	[25]
Ru $3d_{5/2}$	280.1, 280.5, 281.0	Ru–O_{ad}, Ru–$2O_{ad}$, Ru–$3O_{ad}$	[22]
	280.5–280.6	RuO_x	[14]
O 1s	530.0	O_{ad} and RuO_x	[14,22]
O 1s	529.5	O in RuO_2	[25]
O 1s	530.4	OH_x on RuO_2	[26]
O 1s	531.2	CH_3O_x on RuO_2	[26]
O 1s	532.2	CH_2O_x on RuO_2	[26]
O 1s	532.8–533.3	CH_3OH_x on metals	[27]
O 1s	530.6–531.9	CO_x on Ru	[28,29]

3. Results

The evolution of the catalyst chemical state and adlayer composition and the corresponding catalyst activity were studied for different temperatures and partial pressures of O2 and CH3OH in the 10_6 to 10_1 mbar range. Most of the experiments were carried out at oxygen potentials supposed to favour partial oxidation reactions, particularly focused on the selective oxidative dehydrogenation to formaldehyde, the product of industrial importance. As reported below sensible formaldehyde production was monitored only in the 10_1 mbar range and conditions for high selectivity were obtained at T > 450 K for O2/CH3OH molecular mixing ratio (MMR) of 0.6. Since it is naı¨ve to narrow the pressure gap by maintaining a constant O2/CH3OH partial pressure ratio experiments varying the MMR were performed as well.

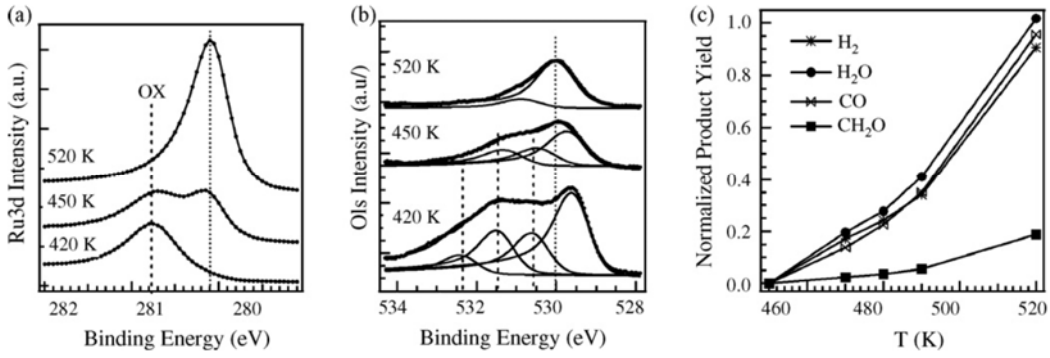

Fig. 2: Ru $3d_{5/2}$ (a) and O 1s (b) spectra corresponding to different reaction temperature for MMR of 0.3 at $P_{total} = 1.8 \times 10^{-1}$ mbar. In (a) and dotted lines indicate oxide and bulk metallic Ru component. In (b) the dashed lines from left to right indicate the O 1s energy positions of CH_2O_s, CH_3O_s and OH_s or CO_s and the dotted line indicates the component of adsorbed oxygen. (c) Mass spectra normalized intensity of reaction products as a function of temperature

Fig. 1(a and b) shows the O 1s and Ru $3d_{5/2}$ spectra of the oxidised pre-catalyst in the 10^{-6} mbar range measured at different temperatures for MMR of 0.6 and following decrease of MMR to 0.25 at 520 K. The O 1s and Ru $3d_{5/2}$ spectra before exposure to the reactants mixture correspond to the RuO_2 state (peaked at _529.5 and 280.8 eV). The O 1s spectrum undergoes significant changes after introducing the CH_3OH reactant. The broad multi-component feature growing on the high-energy side of the O 1s spectra results from the OH_s and CH_xO_s ad-species, derived from CH_3OH dissociative adsorption. The O 1s components giving the best fit of the O 1s spectra in Fig. 1(a) are in fair agreement with the binding energies of OH_s, CH_3O_s and CH_2O_s species on a RuO_2(110) surface (see Table 1). The attenuation and extinction of these O 1s components in the 390–500 K range mark desorption of the CH_3OH-related ad-species. The small shift of the component assigned to OH_s at 390 and 460 K may be due to overlap with the emerging CO_s component resulting from further dehydrogenation of CH_xO_s species. At MMR = 0.6 the oxide catalyst state is preserved up to temperatures of ~ 470 K. At 480 K the measured Ru $3d_{5/2}$ spectrum is still dominated by the RuO_2 component but it starts to broaden on the low energy side due to the emergence of a component at ~280.5 eV of the partially reduced RuOx phase. Above this temperature the Ru bulk component also emerges in the Ru $3d_{5/2}$ spectra indicating sensible partial reduction of RuO_2. The presence of RuO_2 and RuOx components in the Ru $3d_{5/2}$ spectrum at 520 K indicates that both phases coexist at this T, P_{O2} , P_{CH3OH} space, the fraction of the RuO_2 surface being still dominant. At T ~ 460– 480 K the components of the CH_3OH-related almost disappear and the O 1s spectra at 520 K have components corresponding to oxide, RuOx and the weakest component at ~ 531 eV is most likely CO_s. At T ≥ 450 K small CO_2 and H_2O production with almost constant yields in the ~ 490–520 K range was detected, declining with time at 520 K (see Fig. 1(c)). Apparently under the specific reaction conditions only total oxidation is taking place on the oxide catalyst, which is consistent with the presence of traces of CO_s, the only species detected at T > 480– 520 K. Most likely the isothermal decline in the CO_2 and H_2O production at 520 K with time (about 15 min in our experiment) is due to partial reduction of the active RuO_2 catalyst surface. The Ru $3d_{5/2}$ and O 1s spectra evidence that further increase of P_{CH3OH} to get MMR of 0.25 leads to a very fast reduction of RuO_2 into metallic Ru with some adsorbed oxygen. The two spectra in the top panel in Fig. 1(a and b) were measured ~ 1 (bottom) and 5 min after the P_{CH3OH} increase. The attained catalyst steady-state under this new MMR condition is characterised by the appearance of a weak surface component in the Ru $3d_{5/2}$ spectra at 279.5 eV, which indicates that the oxygen coverage drops below 0.5 ML [22], and according to the O 1s spectra these are the only ad-species present under steady conditions. The oxide reduction also changes the catalyst selectivity towards CO, H_2 and H_2O products, as illustrated by the plots in Fig. 1(c). As can be expected, the dramatic change in the catalyst chemical state from oxide to metal affects the overall catalytic activity as well. Comparing the relative methanol consumption (attenuation mass 31 signal) we evaluated that the conversion of methanol on Ru oxide (MMR = 0.6) is ~ 8%, whereas on the metal catalyst (MMR = 0.25) it grows to ~ 29%. Considering the higher P_{CH3OH} the total number of converted methanol molecules at MMR = 0.25 is about nine times higher.

Very similar reduction of the RuO_2 to metallic Ru, which catalyzes the same partial oxidation reaction to CO + H_2O + H_2 was observed for MMR < 0.5 up to mbar reactant partial pressures (see Fig. 2). However, the increase of the reagent pressures by several orders of magnitude leads to the following expected effects, manifested by the differences in the Ru $3d_{5/2}$ and O 1s spectra measured at the 10^{-6} and 10^{-1} mbar: (i) the RuO_2 catalyst undergoes reduction to metallic Ru at lower temperature (already at ~ 460 K); (ii) the coverage of the CH_3O_s and CH_2O_s species on the oxide precatalyst increases, as judged by the higher intensity of the corresponding O 1s components at ~ 531.4 and 532.2 eV; (iii) in addition to oxygen the ad-layer at 520 K contains some CO_s, indicated by the second component at ~ 531 eV in the O 1s spectra; (iv) the overall methanol conversion on the metallic Ru in the 10^{-1} range at 520 K and

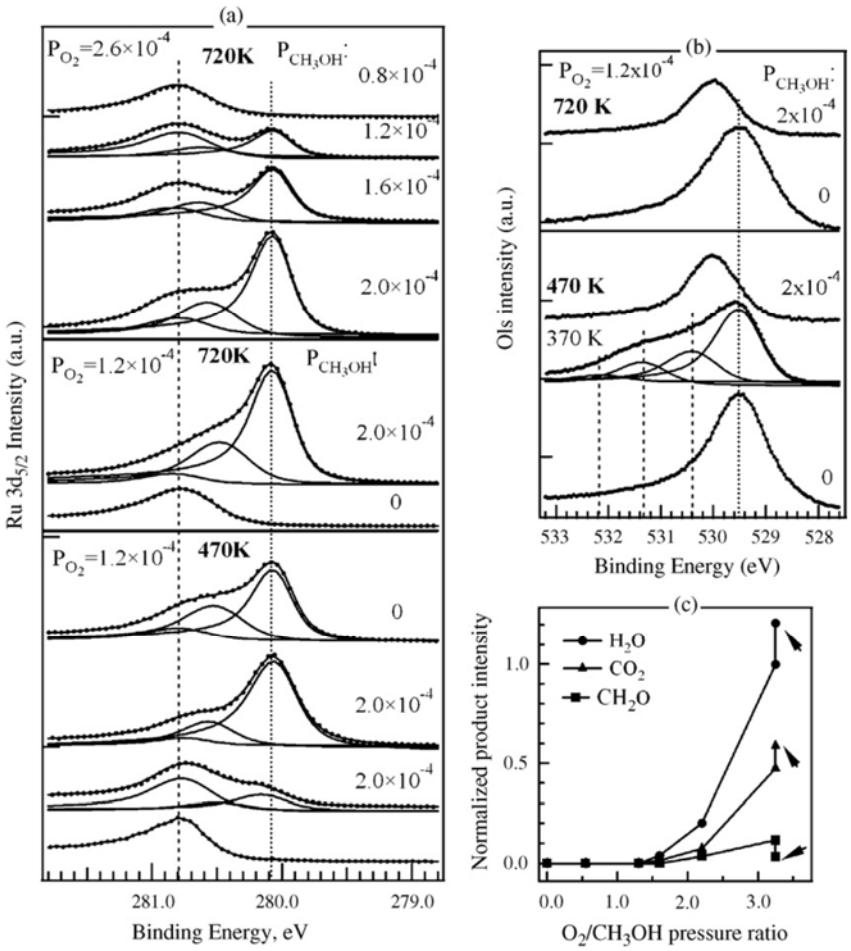

Fig. 3: (a) Ru $3d_{5/2}$ spectra taken at 470 K (bottom panel) and 720 K (mid panel) showing the evolution of the Ru chemical state at constant P_{O2} = 1.2 × 10^{-4} mbar for P_{CH3OH} = 2.0 × 10^{-4} (MMR = 0.6) and 0 mbar. The top panel shows the re-oxidation at 720 K with increasing MMR from 0.6 to 3.3 by varying the P_{O2} and P_{CH3OH}, as indicated in the panel. (b) O 1s spectra corresponding to the Ru 3d5/2 spectra in the bottom and mid panel of (a). The dashed lines from left to right indicate the O 1s energy positions of CH_2O_s, CH_3O_s and OH_s or CO_s and the dotted line indicates the oxide component. (c) Normalized mass spectra intensity of reaction products as a function of MMR at 720 K corresponding to the evolution of the Ru $3d_{5/2}$ spectra in the top panel of (a), where PO2 is 2.6 × 10^{-4} mbar and P_{CH3OH} varies from 2.0 to 0.8 × 10^{-4} mbar. The arrows indicate the change in the products yield after decreasing the temperature to 600 K.

MMR = 0.3 was ~ 20%, i.e. considering the P_{CH3OH} the number of the converted molecules is about 3 orders of magnitude higher compared to almost the same reaction pathway in the 10^{-6} range. At the 10^{-1} mbar pressure range we also detected very small production of CH_2O at 520 K (see Fig. 2(c)), indicating that the competing reaction channel to formaldehyde production is opening at high temperatures.

Further-on, we will focus exclusively on the pressure dependence observed for MMR of 0.6, which was found to favour the CH_2O production in the 10^{-1} mbar range, the highest pressures used in our experimental set-up. The Ru $3d_{5/2}$ and O 1s spectra in Fig. 3 shows that in the 10^{-4} mbar range the RuO_2 pre-catalyst undergoes partial reduction already at 470 K. The Ru $3d_{5/2}$ and O 1s spectra of the reduced state have the characteristic features of the RuOx 'surface oxide'. In accordance with our previous studies [14] the RuO_2 state cannot be restored at 470 K, but the amount of incorporated oxygen (reflected by the weight of RuOx component) can significantly increase after switching-off the CH_3OH flow. The oxide reduction becomes more efficient at higher temperatures (720 K), as evidenced by the spectra in the mid-panel in Fig. 3(a) and top panel in Fig. 3(b). For the 10^{-4} pressure range and MMR = 0.6 the only significant reaction at 470 K and 720 K was the oxide partial reduction to RuOx surface oxide state, which is apparently catalytically inactive at these low oxygen and methanol potentials.

The catalyst can be activated in the 10^{-4} range if it is reoxidised to RuO_2, which takes place at temperatures above 600 K by increasing the MMR, as illustrated by the Ru $3d_{5/2}$ spectra in the top panel in Fig. 3(a). However, as expected the steady RuO_2 state at high MMR catalyzes the undesired total oxidation reaction to H_2O + CO_2, as shown in Fig. 3(c). At MMR above two very low production of CH_2O was also detected at 720 K. Reducing stepwise the temperature the H_2O and CO_2 yields pass through a maximum at 600 K, the CH_2O yield drops almost to zero (see

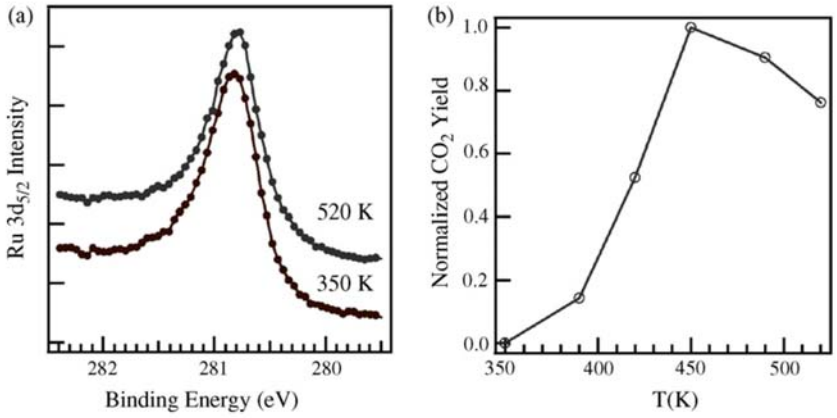

Fig. 4: (a) Ru $3d_{5/2}$ spectra taken during the CO + O_2 reaction illustrating the preserved RuO_2 state for reaction temperatures 350–520 K. (b) Normalized CO_2 mass spectra intensity as a function of temperature. $P_{O2} = 1.6 \times 10^{-4}$ and $P_{CO} = 4.0 \times 10^{-4}$ mbar.

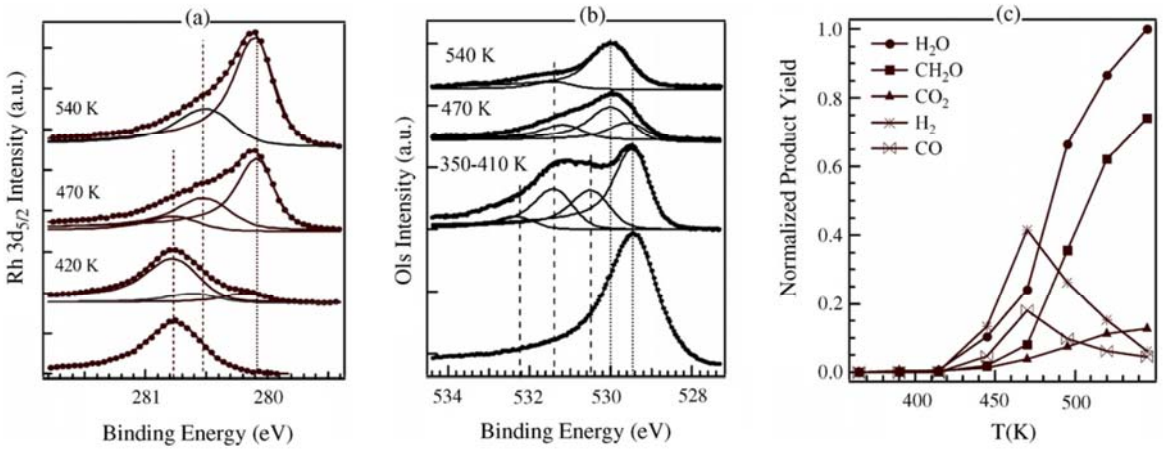

Fig. 5: Ru $3d_{5/2}$ (a) and O 1s (b) spectra at different reaction temperatures for MMR = 0.6 at $P_{total} = 1.8 \times 10^{-1}$ mbar. In (a) and dashed lines indicate the RuO_2 and RuOx components and the dotted line the bulk metallic Ru. In (b) the dashed lines from left to right indicate the O 1s energy positions of CH_2O_s, CH_3O_s and OH_s or CO_s, and the dotted lines the adsorbed oxygen and oxide components. (c) Normalized mass spectra intensity of the reaction products.

the last points in Fig. 3(c) indicated by arrows) and the total methanol conversion increases from 41% at 720 K to 48% at 600 K and MMR = 3.3.

Comparison with the behaviour of the oxidised pre-catalyst during CO oxidation demonstrates the lower stability of the RuO_2 state in O_2 and CH_3OH environment for the sameMMR in the 10^{-4} pressure range. This is due to the release of the very efficient reducing agent H during CH_3OH decomposition. The Ru $3d_{5/2}$ spectra in Fig. 4(a) for reaction temperature from 350 to 520 K show that the oxide catalyst resists reduction down to O_2/COMMR of 0.4. As shown in Fig. 4(b) in this temperature range and MMR the RuO_2 is very active for CO oxidation with a maximum CO_2 yield at 450 K. The decline in the CO_2 yield at higher temperatures can tentatively be ascribed to the stability of adsorbed CO and/or cus-oxygen, in fair agreement with the calculated transition temperature, 450 ± 50 K, for O-cus to O-bridge terminated RuO_2(110) surface at low pressures [30]. In the case of CH_3OH for the same pressure range the RuO_2 undergoes partial reduction already at 470 K even in O_2-richer mixture. Since the O1s spectra indicated that the steady-state adspecies concentration at T > 450 K is very low (i.e. adsorption–desorption processes of reactant and products is very fast) the different T, P_{O2} stability ranges of RuO_2 during CO and CH_3OH oxidation is a direct illustration of the stronger effect of methanol chemical potential. This result holds for high pressures as well.

The results in Fig. 5(a and b), obtained for MMR = 0.6 in the 10^{-1} mbar pressure range, show that the oxidised pre-catalyst undergoes similar partial reduction to RuOx as in the 10^{-4} mbar range, but for these reactant's pressures and T > 470 K the RuOx exhibits the desired catalyst selectivity to the reaction channel $CH_3OH + ½\ O_2 = CH_2O + H_2O$. The catalyst performance with stepwise increasing temperatures, illustrated in Fig. 5(c) shows that in the temperature range of the on-going

partial reduction (420–470 K) only the products of nonselective oxidative dehydrogenation, H_2O, H_2, CO and CO_2 are detected in the gas phase. After each temperature ramp their yields decayed fast (~ 2 times) during the isothermal period and the plots in Fig. 5(c) shows the steady mass signal after the decay. The isothermal decay correlates with the changes in the catalyst surface, which according to the Ru $3d_{5/2}$ and O 1s spectra in Fig. 5(a and b) involve partial reduction and desorption of the CH_3OH-related ad-species. The steady states for the 420–470 K range can be described as coexisting oxide and surface oxide regions with strongly decreased concentration of ad-species. Complete extinction of the oxide component was observed at ~ 490 K and above this temperature the catalytically active state has only the spectral features of the RuOx surface oxide. Above 470 K the yields of the CH_3OH dehydrogenation products (H_2 and CO) drop, whereas the H_2O and CO_2 yields continue growing. The desired product CH_2O appears at ~ 470 K, the H_2O and CH_2O become the principle reaction products above 500 K and at 540 K the total methanol conversion reaches 28%. The binding energy of the second weak component in the O 1s spectra suggests that under steady conditions at 540 K only very small concentration of CH_3O_s species is present on the surface.

More light about the origin of theH_2O,H_2,COandCO_2 yields at temperatures below 480 K is obtained from a 'TPD-type' experiment performed at the same reactant pressures, ramping continuously the temperature with 5°/min and monitoring in situ the mass and Ru $3d_{5/2}$ spectra. The XPS spectra confirm the conversion of the RuO_2 to RuOx in the temperature range 420– 500 K (Fig. 6(a)). The 'TPD'-like mass spectra in Fig. 6(b) can result from several competing reactions: recombination of OH_s to H_2O + H_s, decomposition of the CH_xO_s to CO_s and H_s, and following secondary oxidation of fraction CO_s and H_s to CO_2 and H_2O, the other CO_s and H_s fraction desorbing as CO and H_2 in gas phase. The fact that the CO_2 and H_2O maxima are shifted to higher temperature with respect to that of H_2 and CO ones indicates that H_2O and significant amount of CO_2 are formed via secondary reactions. Another competing viable pathway of CO_2 + H_2O formation is via $CH_{x=2,3}O_s$ + $O_s \rightarrow$ H-$HCOO_s$ + (x-1)$H_s \rightarrow CO_2$ + H_s, where H_s can desorbs as H_2 or interacts with OH_s and desorbs as H_2O. We cannot exclude contribution of this reaction to the mass spectra in Fig. 6, because the classical TPD experiments of methanol adsorption on RuO_2 showed that some CH_2Os species are present on the surface up to 450 K and can undergo dehydrogenation/oxidation to $HCOO_s$, according to the scheme above [26,31]. The 'TPD' results are also in excellent agreement with the O 1s spectra in Fig. 5, which clearly show that the components related to CH_xO_s and OH_s species are stable up to 410 K and only some traces of CH_3O_s remain at 540 K. As for the experiments in the 10^{-4} pressure range, in the same temperature range the RuO_2 catalyst undergoes partial reduction, because the reactive desorption of the CH_xO_s and OH_s species is accompanied by dynamic CH_3OH re-adsorption from the gas phase, as confirmed by the continuous consumption of CH_3OH in the gas phase. Apparently, under the actual reaction conditions the consumption of O_s via reactive oxidative desorption of H_s and CO_s cannot be compensated by the O_2 adsorption and the oxide catalyst undergoes partial reduction. From the relative attenuation of the mass signal at 31 we evaluated that the conversion of methanol of non-selective oxidation at ~ 470 K is ~ 11%, which almost coincides with the consumption measured during step-wise heating ~ 10%.

4. Discussion

The present results evidence a ''pressure gap'' in the CH_3OH selective oxidation, which has no simple explanation as in the case of CO oxidation on Ru(0001), where the activation of the metallic catalyst by oxidation is kinetically limited by the low oxygen potentials at $P_{O2} < 10^{-4}$ mbar. Here, starting with an oxide pre-catalyst we observed significant differences in the selectivity for CH_3OH oxidation at low and high pressures. At given T the reactions depend on the relative methanol and oxygen chemical potentials, which control the catalyst chemical state and adsorbed reactant species. The products of the two non-selective reaction channels, full oxidation to CO_2 + H_2O or partial oxidation to CO + H_2O + H_2 were observed in the whole pressure range considered in the present study, provided the partial reactants pressures and temperatures are properly chosen. Considering the methanol conversion even though measured under significantly different reaction we can conclude that the oxide exhibits high activity for non-selective full oxidation under reaction conditions preserving the RuO_2 surface, high P_{O2}=P_{CH3OH} ratio or lower T (see Figs. 1 and 3). Under this conditions desorption of a small fraction of CH_2O_s before converting to $HCOO_s$ or dehydrogenating to CO_s (further-on $HCOO_s$ decomposes or CO_s oxidises to CO_2) can occur only at rather high T (720 K), resulting in the traces of CH_2O production. The drop of CH_2O production to zero at 600 K (see Fig. 3) confirms such scenario. Lowering the high P_{O2}=P_{CH3OH} ratio affects the stability of the RuO_2 pre-catalyst structure and depending on the actual pressure ratio RuO_2 undergoes partial reduction to a RuOx surface oxide or full reduction to metallic Ru. The metallic Ru state catalyzes effectively only non-selective partial oxidation to CO, H_2O and H_2 in the whole pressure range under consideration.

The intriguing result of the present study is that even if the conditions of the low-pressure experiments are selected to attain the same catalytically active chemical state as at high pressures not necessarily the desired reaction is catalyzed at low potentials of the reactants. This concerns the RuOx surface oxide state, which becomes active only in the 10^{-1} mbar range catalyzing the selective oxidation to CH_2O at T > 450 K. As evidenced by the Ru $3d_{5/2}$ and O 1s spectra in Fig. 5 starting from a RuO_2 pre-catalyst the partial reduction to the RuOx surface oxide precedes the onset of selective CH_2O production. The fits of the Ru $3d_{5/2}$ spectra in Figs. 5 and 6 clearly show that both states, RuO_2 and RuOx, coexist in a wide temperature range, which points

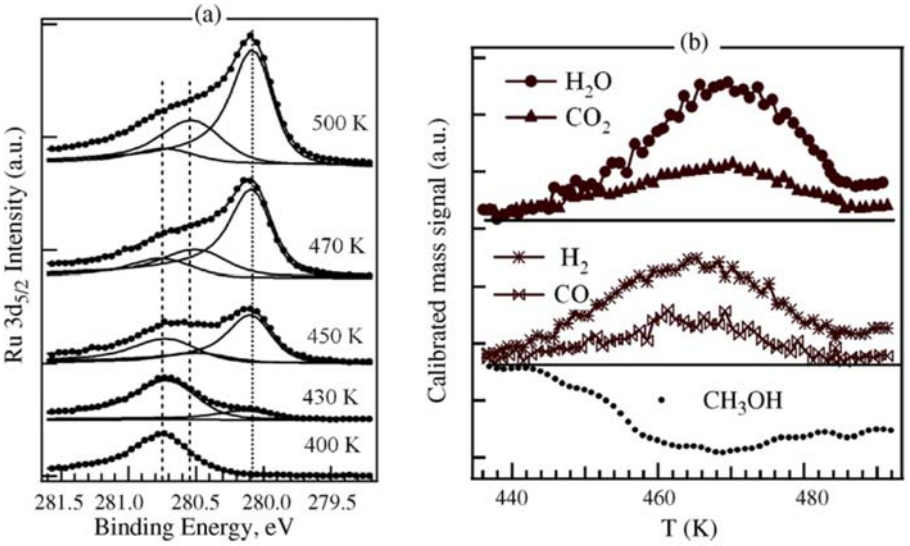

Fig. 6: Evolution of the Ru $3d_{5/2}$ spectra (a) and normalized mass spectra intensity of reaction products (b) monitored during continuous increase of temperature by 5 K/min for MMR = 0.6 at $P_{total} = 1.2 \times 10^{-1}$ mbar. The dotted line in (b) shows the attenuation of mass 31, a measure of CH_3OH conversion.

towards a patchy surface. Above 500 K the RuO_2 component is practically absent and the weight of the RuOx-related component characterises the catalytically active state as a thin few layer surface oxide with poorly defined stoichiometry and structure.

A plausible reason for the observed pressure gap in RuOx activity to CH_2O formation should be kinetic limitations to get the optimal coverage of the reacting species with specific adsorption configurations favouring the CH_2O production. Undoubtedly, the RuO_2 reduction process involving a massive mass transport and restructuring can result in built-up of strain and/or surface roughening and the degree of such dynamic morphological changes may generate configurations with specific reactivity, related to a specific T, P space. This may also determine the critical amount of incorporated oxygen, which selectively activates the catalyst surface to build the optimum surface coverage of the reacting species for the desired reaction channel. Consequently, the high catalyst selectivity should be observed only in a narrow T, P_{O2}, P_{CH3OH} space providing the most favourable energetics of interlinked processes of adsorption, desorption, surface diffusion andsurface reactions. For the reaction system under consideration the crucial intermediate steps relevant to CH2O production are the following:

$$CH_3OH + O_s \rightarrow CH_3O_s + OH_s \quad (1)$$

$$CH_3O_s \rightarrow CH_2O_s + Hs \rightarrow CH_2O_{gas} + H_s \quad (2)$$

$$CH_2O_s + O_s \rightarrow HCOO_s + H_s \rightarrow CO_2 + H_s \quad (3)$$

$$CH_2O_s + O_s \rightarrow CO_s + H_s \text{ and/or} OH_s \quad (4)$$

In our experiments reaction (2) is slower than (1), which sustains some low concentration of CH_3O_s, the only ad-species detected under steady conditions at 540 K. Apparently the catalytically active state should promote reaction (2) with immediate CH_2O_s desorption. If the CH_2O_s lifetime on the surface is long enough it can undergo further oxidationdehydrogenation reactions, types (3) and (4), which favour CO_2 or CO pathways. The most plausible explanation is to correlate the selective CH_2O production to the thermal stability of CH_2O_s. CH_2O_s can be bonded to the surface in two configurations, single-bonded trough the O lone pair orbital, or double-bonded via C and O atoms through carbonyl porbital, the latter being the more stable one [19]. The less stable single-bonded configuration is the preferred one in the presence of oxygen. Therefore one can easily envision that optimal amount of oxygen present at the surface can critically affect the product selectivity not by direct participation in the reaction but via modification of the surface electronic properties and destabilizing adsorbate-adsorbate interactions, which tune the kinetics of CH_2O desorption.

5. Conclusions

In situ XPS and mass spectrometry shed light on the sensitivity of competing methanol oxidation pathways to the ‘pressure gap’, starting with and Ru oxide pre-catalyst and varying the partial reactants pressure from UHV to mbar range. We found that the three main oxidation channels, namely total oxidation to $CO_2 + H_2O$, partial oxidation to $CO + H_2O + H_2$ and partial oxidation to $CH_2O + H_2O$, require completely different catalyst chemical states, which develop only under specific T, P_{O2}, P_{CH3OH} reaction conditions. For all oxygen/ methanol partial pressure ratios used in the present study only the formaldehyde production

is hindered at low pressures, with exception of some traces detected at T > 600 K.

In the whole pressure range under consideration the RuO_2 phase is found to be stable only in the O_2-rich mixtures and catalyzes the total oxidation to CO_2 + H_2O. In CH_3OH-rich mixtures and T > 420 K the RuO_2 undergoes reduction even at pressures as low as 10^{-6} mbar and depending on the reactants partial pressures the reduction can terminate at the transient RuOx surface oxide state. The metallic Ru catalyzes the partial oxidation reaction CO + H_2O + H_2, which is also pressure insensible. The RuOx state turned out to catalyse preferentially the formaldehyde production. Although this state can be formed at low pressures it is activated only at 10^{-1} mbar pressures. Such 'pressure gap' in the selectivity was tentatively ascribed to the correlation between oxygen coverage and the lifetime of the CH_2O intermediate at the surface, the optimal conditions being determined by a narrow T, P_{O2}, P_{CH3OH} space.

Acknowledgements

M. Kiskinova thanks AvH foundation for the Award to pursue research in FHI-Berlin in 2004–2005. P. Dudin acknowledges the financial support under Contract No. NMP3-CT-2003-505670 (NANO2). The BESSY staff is acknowledged for their continuous support to perform the present measurement.

References

[1] P. Mars, D.W. van Krevelen, Chem. Eng. Sci. 3 (1954) 41.
[2] J.A. Labinger, K.C. Ott, Cat. Lett. 4 (1990) 245.
[3] H. Bluhm, M. Hävecker, A. Knop-Gericke, E. Kleimenov, R. Schlögl, D. Teschner, V.I. Bukhtiyarov, D.F. Ogletree, M. Salmeron, J. Phys. Chem. B 108 (2004) 14340.
[4] L. Zhou, S. Gunther, D. Moszynski, R. Imbihl, J. Catal. 235 (2005) 359.
[5] C.I. Carlisle, T. Fujimoto,W.S. Sim, D.A. King, Surf. Sci. 470 (2000) 15.
[6] K. Reuter, in: I. Heiz, H. Hakkinen, U. Landman (Eds.), Nanocatalysis: Principles, Methods, Case Studies, Springer-Verlag, 2005.
[7] C. Stampfl, Catal. Today 105 (2005) 17.
[8] A. Soon, M. Todorova, B. Delley, C. Stampfl, Phys. Rev. B 73 (2006) 165424.
[9] H. Over, Y.D. Kim, A.P. Seitsonen, E. Lundgren, M. Schmid, P. Varga, A. Morgante, G. Ertl, Science 287 (2000) 1474.
[10] H. Over,M. Muhler, Prog. Surf. Sci. 72 (2003) 3 (and references therein).
[11] A. Böttcher, H. Niehus, J. Chem. Phys. 110 (1999) 3186; A. Böttcher, H. Niehus, Phys. Rev. B 60 (1999) 14396.
[12] R. Blume, H. Niehus, H. Conrad, A. Böttcher, J. Phys. Chem. B 108 (2004) 14332.
[13] A. Böttcher, U. Starke, H. Conrad, R. Blume, L. Gregoratti, B. Kaulich, A. Barinov, M. Kiskinova, J. Chem. Phys. 117 (2002) 8104.
[14] R. Blume, H. Niehus, H. Conrad, A. Bo¨ttcher, L. Aballe, L. Gregoratti, A. Barinov, M. Kiskinova, J. Phys. Chem. B 109 (2005) 14052.
[15] R. Blume, M. Hävecker, S. Zafeiratos, D. Teschner, E. Kleimenov, A. Knop-Gericke, R. Schlögl, A. Barinov, P. Dudin, M. Kiskinova, J. Catal. 239 (2006) 354.
[16] W. Vogel, N. Alonso-Vante, J. Catal. 232 (2005) 395.
[17] H. Schulenberg, M. Hilgendorff, I. Dorbandt, J. Radnik, P. Bogdanoff, C. Fiechter, M. Bron, H. Tributsch, J. Power Sources 155 (2006) 47 (and references therein).
[18] M.K. Weldon, C.M. Friend, Chem. Rev. 96 (1996) 1391.
[19] M. Mavrikakis, M. Barteau, J. Mol. Catal. A: Chem. 131 (1998) 135 (and references therein).
[20] H. Liu, E. Iglesia, J. Chem. Phys. B 109 (2005) 2155.
[21] D.F. Ogletree, H. Bluhm, C. Lebedev, C.S. Fadley, Z. Hussain, M. Salmeron, Rev. Sci. Instrum. 73 (2002) 3872. S. Lizzit, A. Baraldi, A. Groso, K. Reuter, M.V. Ganduglia-Pirovano, C. Stampfl, M. Scheffler, M. Stichler, C. Keller, W. Würth, D. Menzel, Phys. Rev. B 63 (2001) 205419.
[22] M.P. Seah, Surf. Interf. Anal. 9 (1986) 85.
[23] NIST database, http://srdata.nist.gov/xps/.
[24] H. Over, A.P. Seitsonen, E. Lundgren, M.Wiklund, J.N. Andersen, Chem. Phys. Lett. 342 (2001) 467.
[25] M. Knapp, et al., in preparation (private communications).
[26] S. Günther, L. Zhou, M. Havecker, A. Knop-Gericke, E. Kleimenov, R. Schlögl, R. Imbihl, J. Chem. Phys. 125 (2006) 11479 (and references therein).
[27] A. Schiffer, P. Jacob, D. Menzel, Surf. Sci. 389 (1997) 116.
[28] G. Rotaris, A. Baraldi, G. Comelli, M. Kiskinova, R. Rosei, Surf. Sci. 359 (1996) 1.
[29] [K. Reuter, M. Scheffler, Phys. Rev. B 65 (2001) 35406.
[30] H. Madhavaram, H. Idriss, S. Wendt, Y.D. Kim, M. Knapp, H. Over, J. Amann, E. Löffer, M. Muhler, J. Catal. 202 (2001) 296.